SUPPLEMENTARY MATERIAL

Analytical Methods

Age determinations were carried out at the Minnesota Isotope Laboratory (USA), using multi-collector inductively coupled plasma mass spectrometry technique (MC-ICP-MS, Thermo-Finnigan NEPTUNE), according to the procedures described in Shen et al. (2002). Twenty four samples weighing between 150 and 300 mg were dissolved and equilibrated with a ^{236}U-^{233}U-^{229}Th spike and then separated and purified using methods described in Edwards et al. (1987). Initial ^{230}Th values were corrected with a typical bulk earth ratio, i.e. atomic ratio of $^{230}Th/^{232}Th = 4.4 \pm 2.2$ ppm. U-Th isotopic data and ages are shown in Supplemental Table DR1.

Oxygen isotope ratios are expressed in δ notation, the per mil deviation from the VPDB standard. For example for oxygen, $\delta^{18}O = [(^{18}O/^{16}O)\ \text{sample}/\ (^{18}O/^{16}O)\text{VPDB}) - 1] \times 1000$. For each measurement, approximately 200 μg of powder was drilled from the sample and analyzed with an on-line, automated, carbonate preparation system linked to a Finnigan Delta Plus Advantage at the University of São Paulo. The speleothem reproducibility of standard materials is 0.1‰ for $\delta^{18}O$.

(A)

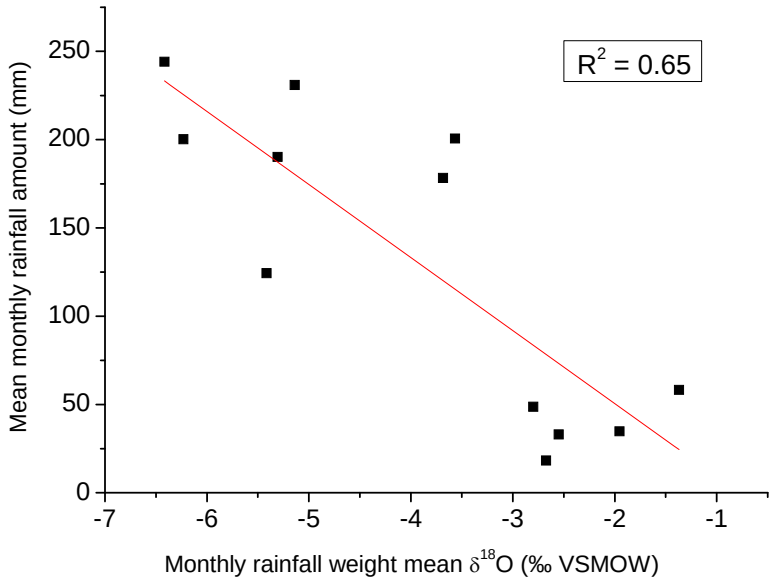

(B)

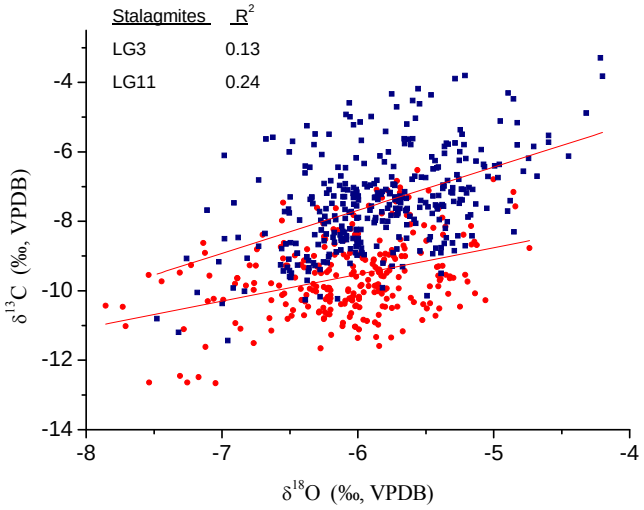

Figure DR1. (A) The relationship between monthly rainwater $\delta^{18}O$ weight mean values and monthly rainfall amount at the IAEA station Brasília (located about 400 km to the southwest from Lapa Grande cave). (B) Scatter diagram of $\delta^{18}O$ versus $\delta^{13}C$ values for each analyzed stalagmite: blue dots indicate LG11 stalagmite and red circles show LG3 stalagmite. The red lines mark the best linear fit. The time intervals covered by each stalagmite are: LG11 from 10.2 to 6.2 ky for LG 11 and from 5.8 to 1.4 ky for LG3.

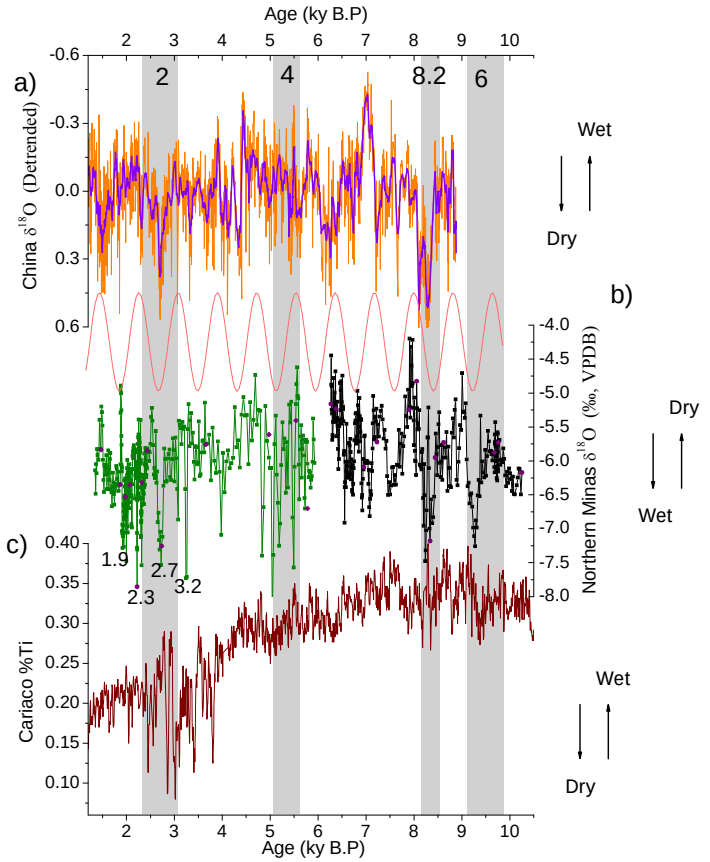

Figure DR2. Comparison between (a) detrended DA stalagmite $\delta^{18}O$ anomalies from Dongge cave, eastern China; purple line indicates a 10 year running mean; (b) Lapa Grande $\delta^{18}O$ record. A sine function in light red is highlighting a cycle of 820 years observed in the spectral analysis of the $\delta^{18}O$ time-series; (c) % Ti from Cariaco basin (Haug et al., 2001) (Wang et al., 2005).

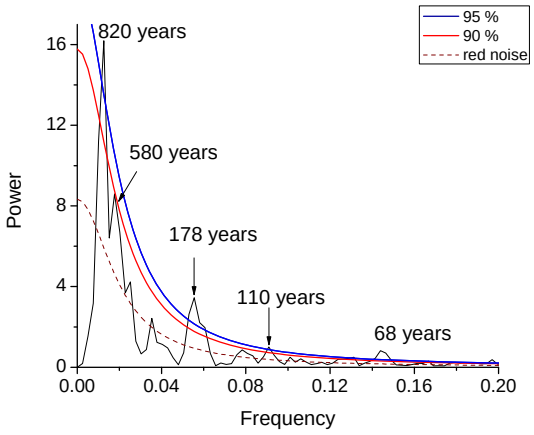

LG11 Stalagmite early and mid-Holocene (10.2 to 6.3 ky B.P)

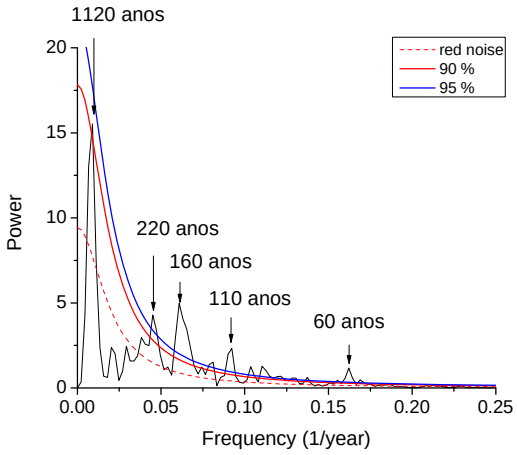

LG3 Stalagmite middle and late-Holocene (5.9 to 1.3 ky B.P)

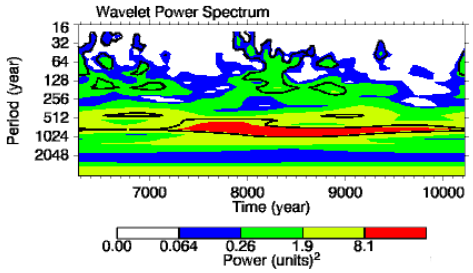

LG11 Stalagmite

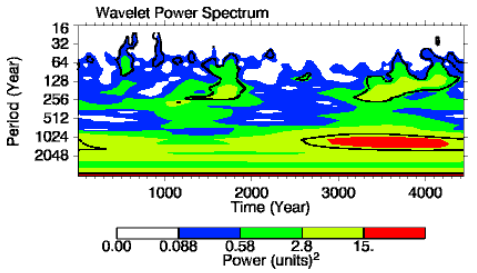

LG3 Stalagmite

Figure DR3. Top: Spectral analysis of the $\delta^{18}O$ time series of LG11 and LG3 stalagmites. Peaks that exceed the 90 % confidence level are labeled with their periods (in years). Analyses were performed with the Past software (Hammer et al., 2001) using the same routine of Schulz and Mudelsee, (2002), which uses the Lomb-Scargle periodogram for unevenly spaced data. Bottom: As on top but for wavelet power spectrum analysis (Torrence and Campo, 1998). The wavelet contours correspond to power levels above 75%, 50%, 25%, and 5%, respectively. Black contours on the wavelet power spectrum indicate the 90% confidence level, using a red-noise (autoregressive lag1) background spectrum. The data were equally spaced at 10 years.

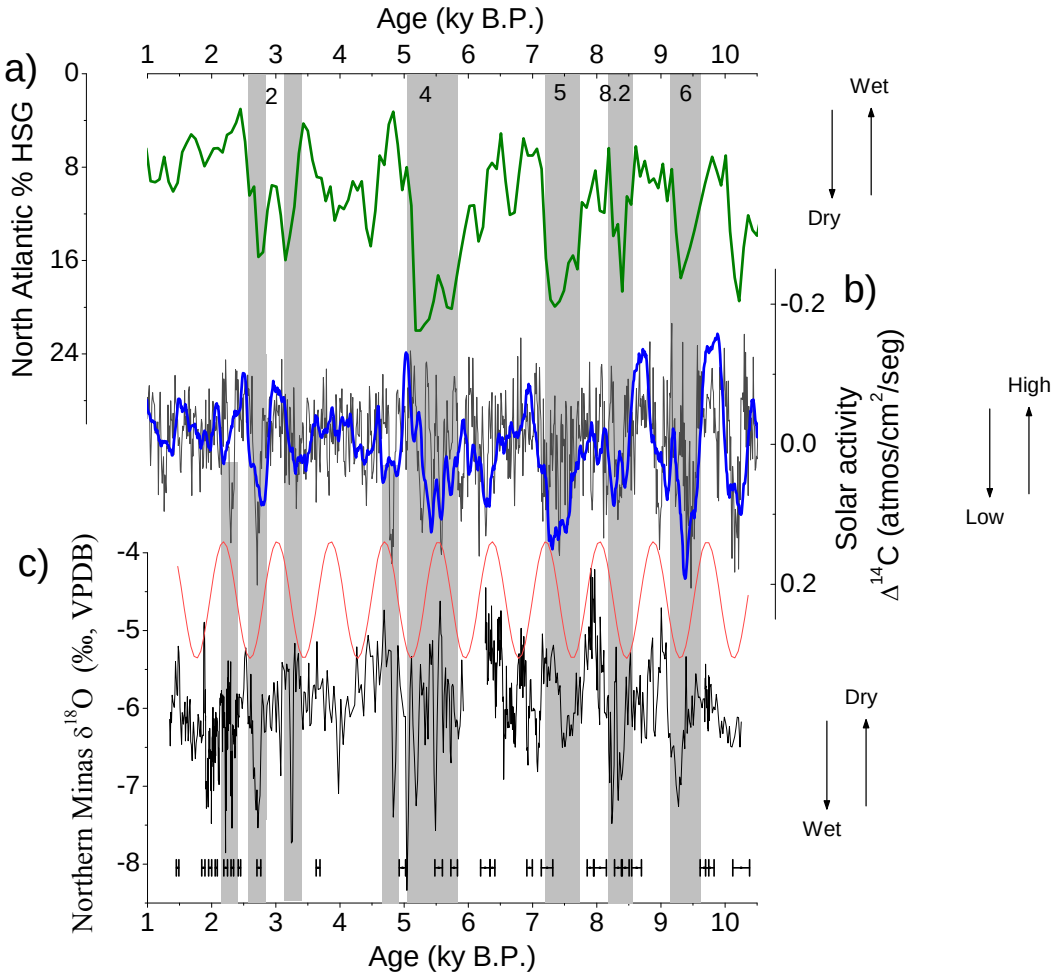

Figure DR4. Comparison between: a) hematite stained quartz grain (HSG) record from North Atlantic of the VM 29-191 (Bond et al., 2001); b) detrended atmospheric $\Delta^{14}C$ on atmos/cm^2/sec (Bond et al., 2001); A 35-year running mean is presented in blue; c) northern Minas LG3 and LG11 stalagmites $\delta^{18}O$ record. The grey bars mark the correspondence between increase in monsoon precipitation and low solar insolation during the events centered at 2.3, 2.7 and 4.8 kyr B.P and in the Bond events 2, 4, 5 and 6 and the 8.2 event.

Supplementary Table DR1. U-Th isotopic data and ages

Sample ID	Dep (mm)	th	^{238}U ppb	^{232}Th ppt	$^{230}Th / ^{232}Th$ (atomic x10^{-6})	$\delta^{234}U$* (measured)	$^{230}Th / ^{238}U$ (activity)	^{230}Th Age (yr) (uncorrected)	^{230}Th Age (yr) (corrected)	$\delta^{234}U_{Initial}$** (corrected)
LG3 - Stalagmite										
LG3-a		6.0	1,356 ± 4	1415 ± 5	349.3 ± 4.2	630.9 ± 3.1	0.02213 ± 0.00027	1,487.16 ± 18	**1,469 ± 20**	634 ± 3.08
LG3-b		25.5	1,231 ± 2.4	258 ± 3	2224 ± 38	655.8 ± 2.2	0.02828 ± 0.00036	1,874.75 ± 24	**1,871 ± 24**	659 ± 2.19
LG3-c		43.5	1,912 ± 4.8	390 ± 3	2387 ± 33	636.4 ± 2.0	0.02953 ± 0.00034	1,981.97 ± 23	**1,978 ± 23**	640 ± 2.03
LG3-d		70.0	1,601 ± 3.6	324 ± 3	2510 ± 30	632.1 ± 1.9	0.03085 ± 0.00024	2,076.46 ± 17	**2,073 ± 17**	636 ± 1.92
LG3-e		84.5	1,714 ± 4.4	219 ± 3	4256 ± 78	633.1 ± 2.1	0.03299 ± 0.00041	2,220.69 ± 28	**2,218 ± 28**	637 ± 2.14
LG3-g		118.0	1,336 ± 2.8	75 ± 3	10302 ± 394	660.4 ± 2.2	0.03508 ± 0.00030	2,323.10 ± 20	**2,322 ± 20**	665 ± 2.18
LG3-h		132.0	1,729 ± 3.2	115 ± 3	8664 ± 221	583.6 ± 1.6	0.03505 ± 0.00026	2,435.03 ± 19	**2,434 ± 19**	588 ± 1.65
LG3-i		143.0	773 ± 3.9	125 ± 3	4071 ± 98	604.2 ± 6.0	0.03987 ± 0.00040	2,738.19 ± 29	**2,735 ± 29**	609 ± 6.02
LG3-J		168.5	883 ± 2.3	97 ± 3	8215 ± 244	655.8 ± 3.1	0.05482 ± 0.00041	3,660.60 ± 29	**3,659 ± 29**	663 ± 3.17
LG3k		185.0	645 ± 1.7	170 ± 3	4384 ± 84	572.0 ± 3.7	0.07039 ± 0.00068	4,978.23 ± 50	**4,973 ± 50**	580 ± 3.72
LG3-l		197.0	546 ± 1.1	163 ± 3	4169 ± 84	522.7 ± 2.7	0.07574 ± 0.00078	5,543.20 ± 59	**5,538 ± 59**	531 ± 2.72
LG3-m		207.0	695 ± 1.4	147 ± 3	5841 ± 122	448.5 ± 2.3	0.07508 ± 0.00063	5,783.55 ± 51	**5,779 ± 51**	456 ± 2.32
LG11 - Stalagmite										
LG11-m	4.5	58	±0.1	31 ±1	2328 ±74	345.4 ±1.8	0.07544 ± 0.00085	6,277.48 ±73	**6,266 ±74**	352 ± 1.83
LG11a-3	14.5	110	±0.2	70 ±2	1989 ±44	342.7 ±2.4	0.07657 ± 0.00043	6,388.32 ±38	**6,375 ±40**	349 ± 2.43
LG11-b	55.5	146 ± 0.4	58 ± 2	3329 ± 91	295.4 ± 4.0	0.08041 ± 0.00040	6,965.16 ± 42	**6,956 ± 42**	301 ± 4.04
LG 11B-5	70.0	75	±0.1	41 ±1	2462 ±88	270.1 ±1.6	0.08178 ± 0.00097	7,240.89 ±89	**7,228 ±89**	276 ± 1.67
LG 11B-5 REPLICATION	70.0	71	±0.1	36 ±1	2720 ±241	280.2 ±1.6	0.08382 ± 0.00672	7,366.73 ±610	**7,355 ±610**	286 ± 1.75
LG 11a-6	87.0	915	±1.3	1326 ±27	996 ±21	244.2 ±2.3	0.08752 ± 0.00045	7,934.94 ±45	**7,901 ±51**	250 ± 2.40
LG11-n	96.0	51	±0.1	37 ±1	2058 ±65	244.2 ±2.3	0.08897 ± 0.00100	8,071.31 ±95	**8,055 ±96**	250 ± 2.32
LG 11B-158	108.5	91	±0.2	40 ±1	3519 ±105	258.3 ±2.0	0.09296 ± 0.00064	8,348.32 ±61	**8,338 ±61**	264 ± 2.10
LG11-p	111.0	55	±0.1	10 ±1	8584 ±453	264.2 ±2.6	0.09451 ± 0.00062	8,450.58 ±61	**8,446 ±61**	271 ± 2.62
LG 11B-7-2	117.5	87	±0.1	37 ±1	3755 ±134	267.0 ±1.9	0.09667 ± 0.00081	8,631.83 ±76	**8,622 ±76**	274 ± 1.99
LG11-d	145.0	64 ± 0.1	54 ± 2	2120 ± 63	273.3 ± 3.3	0.10877 ± 0.00065	9,699.25 ± 66	**9,680 ± 67**	281 ± 3.41
LG 11B-8	160.5	66	±0.1	64 ±1	1842 ±42	268.6 ±2.1	0.10920 ± 0.00065	9,785.73 ±63	**9,763 ±65**	276 ± 2.14
LG11-B	172.5	77 ± 0.1	96 ± 1	1496 ± 28	252.3 ± 3.3	0.11309 ± 0.00134	10,280.36 ± 130	**10,252 ± 131**	260 ± 3.39	

*$\delta^{234}U = ([^{234}U/^{238}U]_{activity} - 1)x1000$.
** $\delta^{234}U_{initial}$ was calculated based on ^{230}Th age (T), i.e., $\delta^{234}U_{initial} = \delta^{234}U_{measured} \times e^{\lambda 234 \times T}$.
Corrected ^{230}Th ages assume the initial $^{230}Th/^{232}Th$ atomic ratio of 4.4 ±2.2 $x10^{-6}$. Those are the values for a material at secular equilibrium, with the bulk earth $^{232}Th/^{238}U$ value of 3.8. The errors are arbitrarily assumed to be 50%.

References cited

Edwards, R.L. , Chen, J.H., and Wasserburg, G.J., 1987, ^{238}U–^{234}U–^{230}Th–^{232}Th systematics and the precise measurement of time over the past 500,000 years: Earth Planetary Science Letters, v. 81, p. 175–192.

Hammer, Ø., Harper, D .A.T., R yan, P.D., 2001, P AST: P aleontological S tatistics Software Package for Education and Data Analysis: Palaeontologia Electronica v. 4, 9pp. http://palaeo-electronica.org/2001_1/past/issue1_01.htm.

Haug, G ., Hughen, K ., S igman, D.M., Peterson, L.C., Röhl, U, 20 01, So uthward migration of the Intertropical Convergence Zone through the Holocene: Science, v. 293, p. 1304-1308, doi: 10.1126/science.1059725.

Shen, C-C., Edwards, R. L., Cheng, H ., D orale, J. A., Thomas, R. B., Moran, S. B., Weinstein, S. E., Ed monds H. N., 2002, Uraniu m and thorium isotopic and concentration measurements by magnetic sector i nductively coupled plasma mass sp ectrometry: Chem ical Geo logy, v. 185, p. 165-178, doi:10.1016/S0009-2541(01)00404-1.

Shulz, M.; Mudel sse, M., 2002, REDFIT: e stimatingred-noise sp ectra d irectly fro m unevenly spaced paleoclimatic time series: Computers & Ge osciences, v. 28, p. 421–426, doi:10.1016/S0098-3004(01)00044-9.

Torrence, C., Compo, G.P., 1998, A Practical Guide to Wavelet Analysis: Bulletin of the American Meteorological Society, v. 79, p. 61-78.

Wang, Y., Cheng, H ., E dwards, R.L., He, Y., Kong, X. An, Z., Wu, J., Kelly , M. J., Dykoski, C. A., Li, X., 2005, The Holocen e Asian Monsoon: Links to solar changes and No rth Atlantic climate, Science, v. 308, p. 8 54-857, do i: 10.1126/science.1106296.